Published online 11 February 2009 *Nucleic Acids Research, 2009, Vol. 37, No. 6* ***2037–2052***
doi:10.1093/nar/gkp064

Characterization of DNA polymerase X from *Thermus thermophilus* HB8 reveals the POLXc and PHP domains are both required for 3′–5′ exonuclease activity

Shuhei Nakane[1], Noriko Nakagawa[1,2], Seiki Kuramitsu[1,2,3] and Ryoji Masui[1,2,*]

[1]Department of Biological Sciences, Graduate School of Science, Osaka University, 1-1 Machikaneyama-cho, Toyonaka, Osaka 560-0043, [2]RIKEN SPring-8 Center, 1-1-1 Kouto, Sayo-cho, Sayo-gun, Hyogo 679-5148 and [3]Systems and Structural Biology Center, Yokohama Institute, RIKEN, 1-7-22 Suehiro-cho, Tsurumi-ku, Yokohama 230-0045, Japan

Received November 4, 2008; Revised and Accepted January 23, 2009

ABSTRACT

The X-family DNA polymerases (PolXs) comprise a highly conserved DNA polymerase family found in all kingdoms. Mammalian PolXs are known to be involved in several DNA-processing pathways including repair, but the cellular functions of bacterial PolXs are less known. Many bacterial PolXs have a polymerase and histidinol phosphatase (PHP) domain at their C-termini in addition to a PolX core (POLXc) domain, and possess 3′–5′ exonuclease activity. Although both domains are highly conserved in bacteria, their molecular functions, especially for a PHP domain, are unknown. We found *Thermus thermophilus* HB8 PolX (ttPolX) has Mg^{2+}/Mn^{2+}-dependent DNA/RNA polymerase, Mn^{2+}-dependent 3′–5′ exonuclease and DNA-binding activities. We identified the domains of ttPolX by limited proteolysis and characterized their biochemical activities. The POLXc domain was responsible for the polymerase and DNA-binding activities but exonuclease activity was not detected for either domain. However, the POLXc and PHP domains interacted with each other and a mixture of the two domains had Mn^{2+}-dependent 3′–5′ exonuclease activity. Moreover, site-directed mutagenesis revealed catalytically important residues in the PHP domain for the 3′–5′ exonuclease activity. Our findings provide a molecular insight into the functional domain organization of bacterial PolXs, especially the requirement of the PHP domain for 3′–5′ exonuclease activity.

INTRODUCTION

DNA polymerases are generally classified into seven families, the A, B, C, D, X, Y and reverse transcriptase (RT) ones (1). In these seven families, the study of X-family DNA polymerases (PolXs) is advanced in eukaryotes, especially in mammals. Mammalian PolXs are further classified into six members: DNA polymerase β (Polβ), μ (Polμ), λ (Polλ), σ1 (Polσ1) and σ2 (Polσ2), and terminal deoxynucleotidyl transferase (TdT) (2). Polβ exhibits Mg^{2+}-dependent DNA/RNA polymerase activity in a DNA-template-dependent manner (3) and is involved in base excision repair (BER) (4). Polλ exhibits Mg^{2+}/Mn^{2+}-dependent DNA polymerase activity in a DNA-template-dependent/independent manner (5,6) and is involved in DNA double-strand break repair (DSBR) (7). Polμ exhibits Mg^{2+}/Mn^{2+}/Co^{2+}-dependent DNA/RNA polymerase activity in a DNA-template-dependent/independent manner (8,9) and is involved in DSBR (10) and V(D)J recombination (11). TdT can incorporate nucleotides at 3′-OH in a template-independent manner (12) and is involved in V(D)J recombination. The Polσs are involved in sister-chromatid cohesion (13). Thus, mammalian PolXs are involved in DNA repair and other DNA-processing pathways.

Eukaryotic PolXs are composed of mainly two domains, a PolX core (POLXc) domain at the C-terminus and a BRCA1 (breast cancer susceptibility protein) C-terminal (BRCT) domain at the N-terminus (Figure 1). However, Polβ consists of only a POLXc domain, and Polσs have no POLXc or BRCT domain (14). The POLXc domain possesses polymerase activity and contains two helix-hairpin-helix motifs, which are responsible for sequence-nonspecific DNA binding (15).

*To whom correspondence should be addressed. Tel: +81 6 6850 5434; Fax: +81 6 6850 5442; Email: rmasui@bio.sci.osaka-u.ac.jp

On the other hand, the BRCT domain interacts with other proteins and/or DNA and joins the Ku-XRCC4-DNA ligase IV-DNA complex for DSBR (16,17). Therefore, although all PolXs are single-subunit enzymes, their domain architecture permits them to exhibit multiple biochemical activities.

The recent completion of many bacterial genome sequences revealed the presence of genes encoding PolXs. Sequence analysis of bacterial PolXs revealed that no bacterial PolXs have a BRCT domain, and that many of them have a polymerase and histidinol phosphatase (PHP) domain at their C-termini in addition to a POLXc domain (2). The PHP domain [also called the histidinol phosphatase-2 (HIS2) domain] is conserved in three taxonomic domains, especially in almost all bacteria. The PHP domain is associated with several proteins, such as DNA polymerases or exists as a stand-alone PHP domain protein (18). The crystal structures of several proteins containing a PHP domain were determined to have a distorted $(\beta\alpha)_7$ barrel fold (19–21). The PHP domain of the DNA polymerase III (PolIII) α-subunit from *Thermus aquaticus* possesses a trinuclear metal site, which is composed of conserved residues including histidine and aspartate ones. The PHP domain exhibits sequence and structural similarity to those of enzymes belonging to the metal-dependent amidohydrolase superfamily (18), but exhibits no similarity to the BRCT domain in mammalian PolXs. Thus, bacterial PolXs have a completely different domain structure from eukaryotic PolXs.

Contrary to the case of mammalian PolXs, the study of the cellular and molecular functions of bacterial PolXs has made little progress. There has only been one recent report of biochemical and gene disruption analysis of PolX from *Deinococcus radiodurans* (drPolX), which is a well-known extremophile exhibiting high resistance to desiccation and ionizing radiation. drPolX has Mg^{2+}/Mn^{2+}-dependent DNA polymerase and Mn^{2+}-dependent 3′–5′ exonuclease activities (22,23). The finding of the 3′–5′ exonuclease activity was unexpected because the other PolXs examined so far lack this activity. The fact that the PHP domain, a member of an amidohydrolase superfamily, is missing in mammalian PolXs raises the possibility that the PHP domain is needed for 3′–5′ exonuclease activity. This possibility is supported by the observation that the α-subunit of PolIII from *T. thermophilus* has Zn^{2+}-dependent 3′–5′ exonuclease activity, and this subunit also contains a PHP domain (24). However, a study on drPolX reported that the POLXc domain had 3′–5′ exonuclease activity and the PHP domain had no intrinsic nuclease activity (23). This discrepancy must be addressed because the 3′–5′ exonuclease activity of bacterial PolXs may be important for the DNA repair process. Blasius *et al.* (23) also showed that the 3′–5′ exonuclease activity of drPolX was dependent on Mn^{2+} as a cofactor like its polymerase activity (22). In this regard, however, it should be noted that compared with other bacteria, the intracellular concentration of Mn^{2+} in *D. radiodurans* is very high, which is supposed to be important for the radioresistance inherent to this bacterium (25). Although deletion of the drPolX gene (DR0467) resulted in a significant delay in DSBR and in an increased sensitivity to γ-irradiation (22), this bacterium might use peculiar molecular mechanisms in response to DNA damage (26). Therefore, to verify the cellular and molecular functions of bacterial PolXs, it is necessary to study PolXs from other bacterial species. In particular, fundamental biochemical aspects of the 3′–5′ exonuclease activity as well as the DNA polymerase activity should be addressed.

In this study, we purified PolX of *T. thermophilus* HB8 (ttPolX) and detected Mn^{2+}-dependent 3′–5′ exonuclease activity in addition to Mg^{2+}-dependent DNA/RNA polymerase activity. As a result of analysis of the two domains, POLXc and PHP, we ascribed the polymerase activity of ttPolX to the POLXc domain, the PHP domain having no intrinsic activity by itself under the conditions tested in this study. We showed that the two domains interacted with each other and that a mixture of the two domains exhibited 3′–5′ exonuclease activity. Moreover, we identified nine catalytically important residues for 3′–5′ exonuclease activity in the PHP domain. These findings provide an important insight for identification of the functional domains for the ttPolX activities and the properties of the conserved PHP domain.

MATERIALS AND METHODS

Materials

The DNA-modifying enzymes, including restriction enzymes and LA Taq polymerase, were from Takara Bio Inc., Shiga, Japan. The yeast extract and polypeptone were from Nihon Pharmaceutical Co., Tokyo, Japan. The deoxyribonucleotide triphosphates (dNTPs) and ribonucleotide triphosphates (NTPs) were from Sigma, St Louis, USA. The DNA oligomers were synthesized by BEX Co., Tokyo, Japan. All other reagents used were of the highest grade and commercially available.

Cloning and overexpression

Sequence analysis of the *T. thermophilus* HB8 genome (DDBJ/EMBL/GeneBank AB107660) revealed one ORF, TTHA1150, encoding a protein which belongs to the PolX family. Using this sequence information, we synthesized two primers for amplification of the *ttha1150* gene by PCR. The gene fragment amplified by PCR using LA Taq polymerase was ligated into the pT7Blue T-vector (Novagen, WI, USA) by TA cloning and confirmed by sequencing. Using the NdeI and Bg1II sites, the fragment bearing the target gene was ligated into pET-11a (Novagen). *Escherichia coli* Rosetta(DE3) cells transformed with the resulting plasmid were cultured at 37°C to 1×10^8 cells/ml in 1.5l LB medium containing 50 μg ml^{-1} ampicillin. The cells were then incubated for 5 h in the presence of 50 μg ml^{-1} isopropyl-β-D-thiogalactopyranoside, harvested by centrifugation and stored at −20°C. The gene fragments of the ttPOLXc and ttPHP domains were amplified from the pT7Blue plasmid containing the *ttha1150* gene by PCR using KOD DNA polymerase (TOYOBO, Osaka, Japan) and ligated into the pET-15b expression vector (Novagen). The primer sets used for the ttPOLXc domain were 5′-TATACATATGCGTAACCA

GGAGCTCGCCCGGATC-3′ and 5′-TATAAGATCTT ATTACCGCACCGCCGGGGAG-3′, and those for the ttPHP domain were 5′-TATGAATTCCATATGGGTG ACCTCCAGGTCCACTCC-3′ and 5′-TATGGATCCTT ATTAAACGCCACGACGGGCTTTGAG-3′. Overexpression of the ttPOLXc and ttPHP domains was performed in the same way as for ttPolX except for the use of *E. coli* Rosetta2(DE3)pLysS cells as the expression host.

Protein purification

All the following procedures were carried out at room temperature unless stated otherwise. Frozen cells expressing ttPolX were thawed, suspended in 20 mM Tris–HCl and 100 mM KCl, pH 8.5, and then disrupted by sonication on ice. The lyzate was incubated at 60°C for 10 min and centrifuged (38 900*g*) for 30 min at 4°C. Ammonium sulfate (AS) was added to the resulting supernatant to a final concentration of 1.8 M. Then the solution was centrifuged (38 900*g* for 30 min at 4°C), and the resulting supernatant was applied to a TOYOPEARL Phenyl-650 M column (Tosoh, Tokyo, Japan) and proteins were eluted with a linear gradient of 1.8-0 M AS. The fractions containing ttPolX were applied to a TOYOPEARL SuperQ-650 M column equilibrated with 20 mM Tris–HCl, pH 8.5, and proteins were eluted with a linear gradient of 0–0.5 M NaCl. The fractions containing ttPolX were then applied to a hydroxyapatite column (Bio-Rad, CA, USA) equilibrated with 10 mM sodium phosphate, pH 7.0, and eluted with a linear gradient of 10–500 mM sodium phosphate. The fractions containing the ttPolX were collected and concentrated with a Vivaspin concentrator (molecular weight 30 000 cut-off). The concentrated solution was applied to a Superdex 200 HR 10/30 column (GE Healthcare UK Ltd) equilibrated with 20 mM Tris–HCl and 100 mM KCl, pH 8.5, and eluted with the same buffer using an ÄKTA explorer system. The fractions containing the ttPolX were concentrated and stored at 4°C. Frozen cells expressing the His-tagged ttPOLXc domain (ttPOLXc domain) were thawed, suspended in binding buffer (20 mM Tris–HCl, 500 mM NaCl and 5 mM imidazole, pH 7.9) and then disrupted by sonication on ice. The lyzate was centrifuged (38 900*g*) for 30 min at 4°C. The resulting supernatant was applied to a His·Bind Resin column (Novagen) equilibrated with binding buffer and proteins were eluted with a linear gradient of 5–1000 mM imidazole. The fractions containing the ttPOLXc domain were collected and AS was added to a final concentration of 0.8 M. Then the solution was applied to a TOYOPEARL Butyl column (Tosoh) equilibrated with 20 mM glycine and 0.8 M AS, pH 7.0, and eluted with a linear gradient of equilibration buffer to 20 mM glycine, pH 9.0. The fractions containing the ttPOLXc domain were collected, concentrated and applied to a Superdex 75 HR 10/30 column (GE Healthcare). The purified ttPOLXc domain was stored in 20 mM Tris–HCl and 100 mM KCl, pH 9.1, at 4°C. Purification of the His-tagged ttPHP domain (ttPHP domain) was performed in a similar way to for the ttPOLXc domain but with the use of a TOYOPEARL Phenyl column not a TOYOPEARL Butyl one, with equilibration buffer comprising 20 mM Tris–HCl and 1 M AS, pH 7.4, and elution with a linear gradient of equilibration buffer to 20 mM Tris–HCl, pH 8.5. After each step, fractions were analyzed by SDS–PAGE. The concentration of the purified protein was determined by using a molar extinction coefficient at 278 nm calculated according to the formula of Kuramitsu *et al*. (27). The calculated molar extinction coefficients of ttPolX, ttPOLXc and ttPHP domains were 66 885, 29 190 and 47 880 $M^{-1}cm^{-1}$, respectively. We identified the purified protein as a ttPolX, and the ttPOLXc and ttPHP domains by means of peptide mass fingerprinting (PMF) involving matrix-assisted laser desorption/ionization time-of-flight mass spectrometry (MALDI-TOF MS). Briefly, we measured a mass spectrum of the peptide mixture resulting from the digestion of a protein by trypsin and compared it to the database containing the theoretical mass spectra of tryptic peptide mixtures from each protein encoded in *T. thermophilus* HB8 genome. By statistical comparison between experimentally determined and theoretical mass spectra, we identified each purified protein as a target protein.

Spectroscopic analysis

Circular dichroism (CD) spectra in the far-UV region (200–250 nm) were obtained at 25°C with a Jasco spectropolarimeter, J-720W, using 1.5 μM (ttPolX) or 5 μM (ttPOLXc and ttPHP domains) enzyme in 50 mM potassium phosphate and 100 mM KCl, pH 7.0, at 25°C. Thermostability was investigated by recording the molar ellipticity at 222 nm from 25°C to 95°C under the same conditions as above.

Limited proteolysis

ttPolX (10 μM) was incubated with trypsin (0–100 nM) in buffer comprising 20 mM Tris–HCl, pH 8.0, at 25°C or with thermolysin (0–100 nM) in buffer comprising 20 mM Tris–HCl and 10 mM $CaCl_2$, pH 7.8, at 37°C. After incubation for 1 h, samples were analyzed by 12.5% SDS–PAGE. The N-terminal sequences of peptide fragments were determined using a protein sequencer (Procise HT, Applied Biosystems, CA, USA).

DNA/RNA polymerase assays

Reaction mixtures comprised 20 mM Tris–HCl, 20 mM KCl, 10 μM dNTPs or NTPs, 5 mM $MgCl_2$ or 1 mM $MnCl_2$, 1 μM enzyme and 10 nM oligonucleotides, pH 8.0, at 37°C. The sequences of the oligonucleotides were 5′-CACTGGCGGTCGTTCTATCGGGTGTTGCTTTA GTTGTCAT-3′ (40T), 5′-ATGACAACTAAAGCAACA CCC-3′ (21F), 5′-ATGACAACTAACGCAACACCC-3′ (12C21), 5′-ATGACAACTAAIGCAACACCC-3′ (12I21, I = deoxyinosine), 5′-ATGACAACTAAXGCAACACC C-3′ (12X21, X = deoxyxanthine), 5′-r(AUGACAACUA AAGCAACACCC)-3′ (21RNA) and 5′-GGGTGTTGC-3′ (9P). The assays were performed with 21F/40T (primer/template), 9P/21F (primer/template), 9P/12C21 (primer/template), 9P/12I21 (primer/template), 9P/12X21 (primer/template) or 9P/21RNA (primer/template). We radiolabeled the 5′-end of each primer using [γ-^{32}P] ATP and T4 polynucleotide kinase. The oligonucleotides were

mixed in equimolar and heated at 95°C for 2 min, and cooled gradually for the annealing. The reaction mixtures were incubated for 30 min at 37°C unless stated otherwise and the reactions were stopped by the addition of 2× denaturing dye (5 mM EDTA, 80% deionized formamide, 10 mM NaOH, 0.1% bromophenol blue and 0.1% xylene cyanol), followed by analysis by denaturing PAGE. The gel contained 8 M urea, and electrophoresis was performed with 1 × TBE buffer (89 mM Tris–borate and 2 mM EDTA). The DNA was visualized and analyzed by autoradiography using a Bio-imaging analyzer BAS2500 (Fuji Film).

Exonuclease assays

Reaction mixtures comprised 20 mM Tris–HCl, 20 mM KCl, 1 mM $MnCl_2$, 1 μM enzyme and 10 nM 5′-labeled oligonucleotides, pH 8.0, at 37°C. The oligonucleotides used were 21F and 5′-GGGTGTTGCTTTAGTTGT CAT-3′ (21R). The assays were performed with 21F (single strand) and 21F/21R (double strand). The annealing condition was as described above. The reaction mixtures were incubated for 30 min at 37°C and analyzed as described above. For determination of kinetic parameters, 50 nM ttPolX or 200 nM domain mixture (200 nM ttPOLXc and 200 nM ttPHP domains) was incubated in reaction mixtures comprising 20 mM Tris–HCl, 20 mM KCl, 1 mM $MnCl_2$, 10 nM 3′-labeled 21F, with or without 10 μM dNTPs and 6.25–12 800 nM unlabeled oligonucleotides, 22F (5′-ATGACAACTAAAGCAACACCCA-3′), pH 8.0, at 37°C. Radiolabeling at the 3′-end was performed using TdT (Promega, WI, USA) and [α-^{32}P] cordycepin 5′-triphosphate (PerkinElmer Inc., MA, USA). The reaction mixtures were incubated for 10 min at 37°C and analyzed by 20% denaturing PAGE (8 M urea). The oligonucleotides were analyzed by autoradiography using a BAS2500. Kinetic parameters were calculated by fitting the data to the Michaelis–Menten equation using Igor 4.03 (Wave Metrics, OR, USA).

Site-directed mutagenesis of ttPolX

ttPolX mutants of Q342A, H344A, D349A, H374A, E413A, H440A, H468A, D529A and H531A were obtained by means of the inverse PCR method. PCR was performed using KOD or KOD-Plus-DNA polymerases (TOYOBO) and pET-11a containing the *ttha1150* gene as a template plasmid. PCR products were purified with a RECOCHIP (TaKaRa) and phosphorylated at the 5′-end with T4 polynucleotide kinase. Template plasmid was digested with DpnI restriction enzyme. Phosphorylated PCR products were ligated by self-ligation using T4 DNA ligase and confirmed by sequencing. *E. coli* Rosetta2(DE3)pLysS cells were transformed with the constructed plasmids. Expression and purification of ttPolX mutants were performed as described for the wild-type ttPolX.

Electrophoretic mobility shift assay

Reaction mixtures comprised 20 mM Tris–HCl, 20 mM KCl, 2 mM EDTA, protein and oligonucleotides, pH 8.0, at 37°C. The oligonucleotides used were 5′-ATG ACAACTAAAGCAACACCCGATAGAACGACCGC CAGTG-3′ (40C), 21F, 40T, 5′-ATAGAACGACCGCCA GTG-3′ (18G) and 5′-phosphorylated 18G (P18G). The assays were performed with 40T [single-stranded DNA (ssDNA)], 40T/40C [double-stranded DNA (dsDNA)], 21F/40T/18G (1-nt gapped DNA), or 21F/40T/P18G (5′-phosphorylated 1-nt gapped DNA). In all electrophoretic mobility shift assay (EMSA) analyses, the oligonucleotide of 40T was 5′-radiolabeled, and the oligonucleotides were annealed as described above except for adding three times higher concentration of the oligonucleotides of 18G and P18G to anneal perfectly. The reaction mixtures were incubated for 30 min at 37°C and then mixed with 5 × native dye (5 mM EDTA, 50% glycerol and 0.05% bromophenol blue). The mixtures were loaded onto a 5% polyacrylamide gel, electrophoresed in TBE buffer and analyzed by autoradiography.

When multiple molecules of an enzyme bind to a substrate, the apparent dissociation constant (K_d^{app}) can be represented by the following equation (1):

$$nE+S \underset{}{\overset{K_d^{app}}{\rightleftarrows}} EnS$$
$$K_d^{app} = [E]^n[S]/[E_nS] \quad \mathbf{1}$$

where E is the free enzyme, n the number of binding enzyme, S the free DNA, E_nS the enzyme–DNA complex. Since the substrates were mixed with a large excess of enzyme, the following postulations were applied.

$$[E]_0 = [E] \quad \mathbf{2}$$

$$[S]_0 = [S] + [E_nS] \quad \mathbf{3}$$

where $[E]_0$ is the concentration of total enzyme and $[S]_0$ the concentration of total DNA. Based on equations (1–3), $[E_nS]$ is represented as a function of $[E]_0$.

$$[E_nS] = [E]_0^n[S]_0/([E]_0^n + K_d^{app}) \quad \mathbf{4}$$

The K_d^{app} value was calculated by fitting the data to equation (4) using Igor 4.03 (Wave Metrics).

Size exclusion chromatography

The oligomeric state of ttPolX, the domains and domain mixture in solution was assessed by size exclusion chromatography on Superdex 75 HR 10/30 column (GE Healthcare). A sample contained 20 mM Tris–HCl and 100 mM KCl with or without 10 μM dNTPs, and a protein, pH 8.5, at 25°C. The protein was eluted with the same buffer. The apparent molecular weight was estimated using molecular weight marker proteins (Sigma).

RESULTS

Preparation of ttPolX

The sequence of *ttha1150* encodes ttPolX of 575 amino acid residues. ttPolX has a calculated molecular mass of 64 kDa with a theoretical isoelectric point of 6.3. We overexpressed ttPolX in *E. coli* and purified the

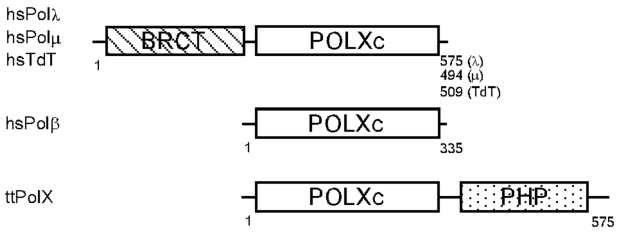

Figure 1. Domain structures predicted by sequence motif analysis of representative PolXs. The numbers represent the amino acid residues. hsPolλ hsPolμ, hsTdT and hsPolβ represent the enzymes of *Homo sapiens*. The accession numbers are as follows: NP_037406 for hsPolλ; NP_037416 for hsPolμ; NP_004079 for hsTdT; NP_002681 for hsPolβ and YP_144416 for ttPolX.

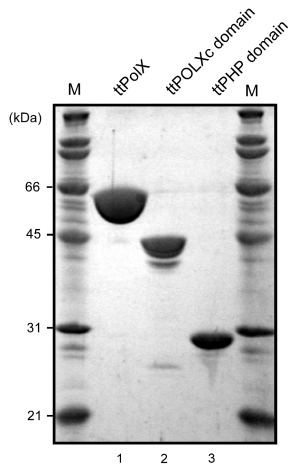

Figure 2. Purified ttPolX and its domains. The purified proteins were analyzed by 12.5% SDS–PAGE and stained with Coomassie Brilliant Blue (CBB). M represents molecular weight markers. The theoretical molecular weights of ttPolX and the His-tagged domains were 64, 44 and 29 kDa, respectively.

protein to homogeneity by means of heat treatment and four column chromatography steps (Figure 2). Approximately 20 mg of ttPolX was obtained from 10 g of cells.

Size exclusion chromatography was performed to investigate the oligomeric state of ttPolX. The apparent molecular mass corresponding to the peak was estimated to be 48 kDa (Table 1), which was less than the mass (64 kDa) calculated from the sequence. This result indicates that ttPolX exists in a monomeric state in solution. The far-UV CD spectrum showed negative double maxima at 209 and 222 nm, characteristic of an α-helical structure (data not shown). Based on the ellipticity at 222 nm, the melting temperature (Tm) of ttPolX was shown to be 75°C (data not shown).

Limited proteolysis of ttPolX

To reveal the organization of the structural domains of ttPolX, we performed limited proteolysis of the purified ttPolX using trypsin and thermolysin. Under mild conditions, endoproteases are expected to preferentially hydrolyze a protein at the sites exposed to the solvent, which are often within interdomain linker regions. As

Table 1. Comparison of the elution volumes

	Elution volume (ml)	A_{280} (mAU)	MW[a]
ttPolX	9.8	32.5	48 k (64 k)
ttPOLXc domain	10.3	9.5	40 k (44 k)
ttPHP domain	11.2	24.9	30 k (29 k)
Domain mixture (1)	9.7	16.7	50 k
Domain mixture (2)	11.3	15.1	29 k
Domain mixture with dNTPs (1)	9.7	19.2	50 k
Domain mixture with dNTPs (2)	11.2	13.4	30 k

[a]The apparent molecular weights were calculated using the following equation: log MW = −0.147 [elution volume (ml)] + 3.12. The MWs given in the parentheses are theoretical values calculated from amino acid sequences. The void volume of this Superdex 75 column measured using blue dextran was 7.8 ml.

shown in Figure 3A, treatment of ttPolX (64 kDa) with trypsin or thermolysin mainly produced two fragments of 42 and 25 kDa. Peptide sequence analysis revealed that trypsin and thermolysin cleaved ttPolX at the same position. The N-terminal sequence of the 42 kDa fragment was MRNQELARIF, which agreed with N-terminal residues 1–10 of ttPolX. The N-terminal sequence of the 25 kDa fragment was VAGGPSPEEA, which agreed with residues 380–389. The calculated molecular masses of the fragments comprising residues of 1–379 and 380–575 were close to 42 and 25 kDa, respectively. In addition, there was further evidence to locate the position of the interdomain linker region. The purified ttPolX was degraded into two fragments of 44 kDa and 25 kDa after cold storage in 20 mM Tris–HCl and 100 mM KCl, pH 9.1, at 4°C for half a year (Figure 3B). The N-terminal sequences of these 44 and 25 kDa fragments were MRNQELA (residues 1–7) and GGPSPEE (residues 382–388), respectively. These results indicated that residues around 380 comprised the interdomain region of ttPolX. The notion that ttPolX is composed of mainly two structural domains is in agreement with the prediction based on sequence motif analysis (Figure 1).

Based on the results of limited proteolysis, we prepared the N-terminal and C-terminal domains as separate protein fragments. The His-tagged N-terminal fragment, corresponding to residues 1–379, was successfully overexpressed in *E. coli* and purified (Figure 2). However, the C-terminal fragment, corresponding to residues 380–575, with or without a His-tag, was hardly overexpressed and could not be purified. Then, we compared the amino acid sequences of the C-terminal regions of ttPolX and *E. coli* YcdX. YcdX is a hypothetical protein comprising a PHP domain alone and its crystal structure has already been determined (19). Several charged residues conserved among PHP domain sequences are coordinated to bound metal ions and thus assumed to be catalytically important residues. Sequence alignment revealed that these residues are well conserved in the C-terminal regions of ttPolX and YcdX (Figure 3C). This alignment showed that the C-terminal domain obtained by limited proteolysis lacks the putative four residues of catalytic importance. Therefore, we reevaluated that the C-terminal domain

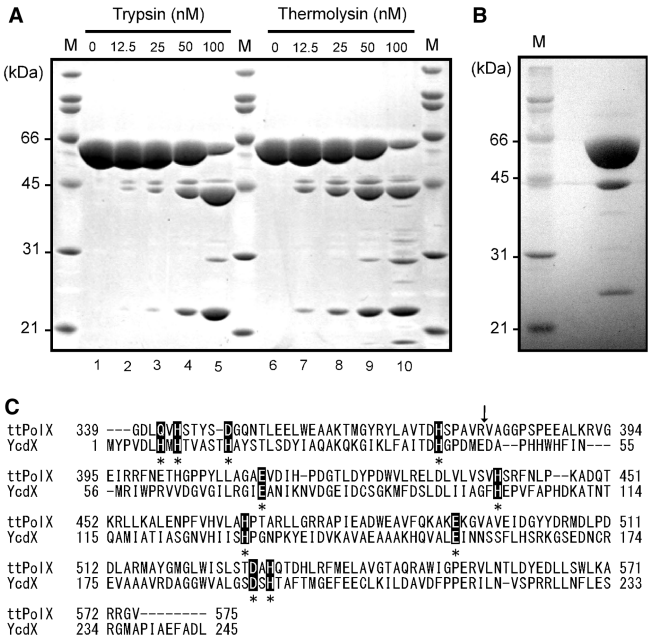

Figure 3. The organization of structural domains of ttPolX. M represents molecular weight markers. (**A**) ttPolX (10 μM) was digested with trypsin or thermolysin under mild conditions and then analyzed by 12.5% SDS–PAGE and stained with CBB. (**B**) ttPolX degraded after cold storage at 4°C for half a year was analyzed by 12% SDS–PAGE and blotted onto a PVDF membrane for peptide sequence analysis, and stained with CBB. (**C**) Sequence alignment of ttPolX and *E. coli* YcdX. The accession number of YcdX is NP_415552. Asterisks (*) indicate putative catalytically important residues for binding to metal ions in the YcdX crystal structure (19). The arrow indicates the cleaved position on ttPolX with trypsin and thermolysin. The alignment was performed with ClustalW2 (28).

comprises residues 339–575 of ttPolX and constructed an expression plasmid containing this region. As a consequence, we succeeded in overexpression and purification of this fragment (Figure 2). In this study, we used these N-terminal (1–379) and C-terminal domains (339–575) to identify functional domains and called them the ttPOLXc domain and ttPHP domain, respectively. The theoretical molecular weight, isoelectric point and Tm estimated from the CD spectrum of the ttPOLXc domain were 42 kDa, pH 8.4 and 70°C, respectively. The corresponding values for the ttPHP domain were 27 kDa, pH 6.0 and 50°C, respectively.

The activities of ttPolX

We found that ttPolX had Mg^{2+}-dependent 5′–3′ DNA/RNA polymerase and Mn^{2+}-dependent 3′–5′ exonuclease activities (Figure 4). Note that the RNA polymerase activity is the DNA primer/template-dependent NMP polymerization activity in this study. In the polymerase assay, we observed that the 5′-labeled primer (21F) binding to the template (40T) was extended in the 5′–3′ direction by ttPolX in the presence of Mg^{2+} (Figure 4A). We also performed polymerase assay with Mn^{2+} because several PolXs are known to have Mn^{2+}-dependent polymerase activity (5,8,22), however, degradation of the primer was observed (Figure 4A, lane 2). Similar degradation was observed for ssDNA with Mn^{2+} but not with Mg^{2+} (Figure 4A, lanes 3 and 4). Such Mn^{2+}-dependent nuclease activity prevented us from determining whether ttPolX had Mn^{2+}-dependent DNA polymerase activity or not. After 240 min, the primer was extended up to the template length of a 40-mer (Figure 4B, lanes 1–6). Figure 4B also shows that ttPolX was able to insert not only deoxyribonucleotide monophosphates (dNMPs) but also ribonucleotide monophosphates (NMPs) (Figure 4B, lanes 7–12). This indicated that ttPolX was able to synthesize RNA against the DNA template, although the RNA polymerase activity was lower than the DNA polymerase activity.

The nuclease activity of ttPolX was further investigated. In the exonuclease assay, we used 5′-labeled 21F as ssDNA or as dsDNA (21F/21R). As shown in Figure 4C, the 5′-labeled oligonucleotides became shorter in the presence of Mn^{2+} with ttPolX as time passed. This result indicated that the direction of the exonuclease activity was 3′–5′. Figure 4C also shows that the exonuclease activity for dsDNA was weaker than that for ssDNA. ttPolX had no polymerase or exonuclease activity with 5 mM Zn^{2+}, Ni^{2+}, Ca^{2+}, Co^{2+}, Fe^{2+}, Sr^{2+}, Mo^{6+}, Vo^{2+} or Cu^{2+}, or without a metal ion (data not shown). Therefore, the intrinsic exonuclease activity of ttPolX was critically dependent on Mn^{2+}.

To estimate the ability of ttPolX to discriminate bases, we examined what kinds of nucleotide ttPolX can insert opposite the template base, dC. When one kind of canonical dNTP or NTP was added to the reaction mixture for the polymerase assay, ttPolX inserted only dGMP and GMP next to the 3′-OH of the primer (21F), indicating that ttPolX preferentially inserted complementary nucleotides for canonical nucleotides (Figure 4D, lanes 1–10). We further examined the incorporation of guanine nucleotide derivatives opposite dC, XTP, dITP, ITP and 8-oxo-deoxyguanosine triphosphate (8-oxo-dGTP) being used as substrates. ttPolX inserted 8-oxo-dGMP, and slightly inserted dIMP and IMP (Figure 4D, lanes 11–14). The observation that ttPolX inserted dGMP, GMP and 8-oxo-dGMP opposite dC indicated that ttPolX synthesizes DNA following the rule of Watson–Crick base-pairing.

ttPolX was unable to insert nucleotides opposite non-canonical bases or RNA. We measured the translesion synthesis (TLS) activity of ttPolX using oligonucleotides 9P/12I21 (containing inosine) and 9P/12X21 (containing xanthine), and RT activity using 9P/21RNA. Because of the low Tm of the 9P primer (Tm = 30°C), we performed the polymerase assay using 9P/21F and 9P/12C21 as a control experiment for confirmation of primer annealing. When 9P/12C21 and dNTPs were used as substrates, extension of the primer was confirmed at 25, 30 and 37°C (Figure 4E, lane 3), and the extension activity was higher at 37°C than at 25 or 30°C (data not shown). Therefore, we performed polymerase assay using 9P as the primer at 37°C. With the use of 9P/12I21, 9P/12X21 or 9P/21RNA, ttPolX inserted neither dNMPs nor NMPs opposite dI (12I21), dX (12X21) or A (21RNA) of the template (Figure 4E, lanes 5–10). These results suggest that ttPolX exhibits no TLS or RT activity in the presence of Mg^{2+}. It should be noted that extension of the primer

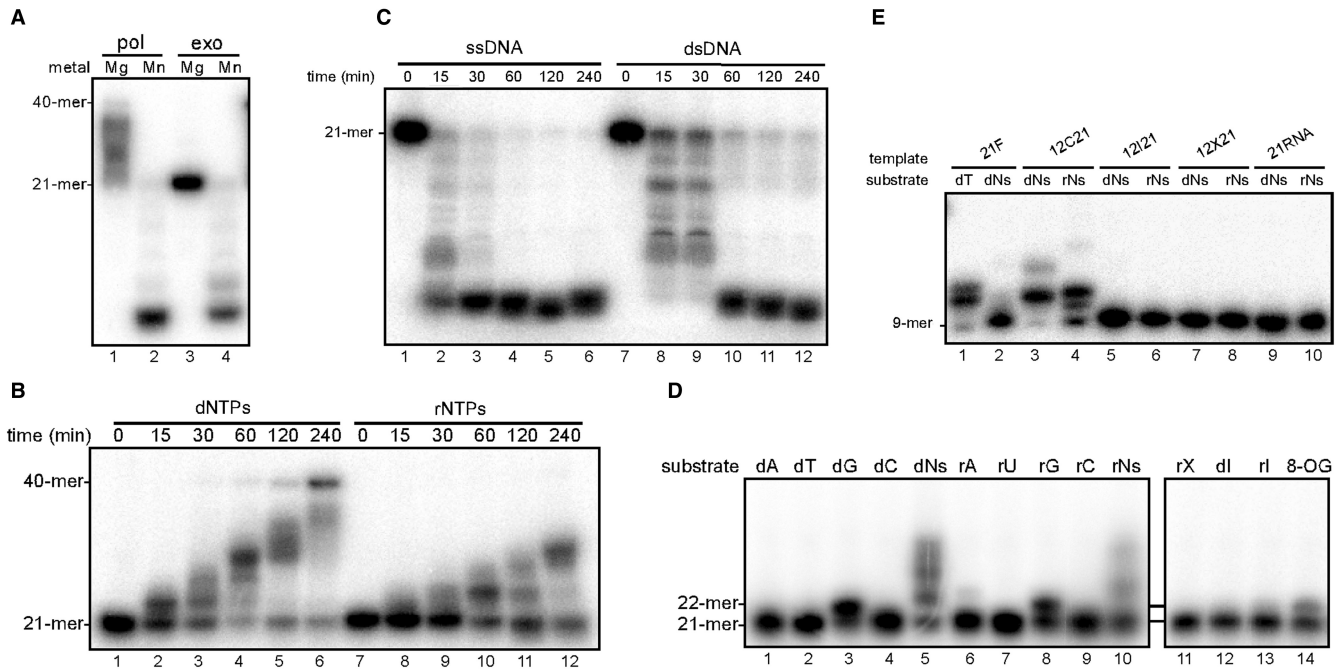

Figure 4. DNA/RNA polymerase and 3′–5′ exonuclease activities of ttPolX. (**A**) Metal ion dependence of the activities in the presence of 5 mM $MgCl_2$ or 1 mM $MnCl_2$. The reaction conditions for the polymerase assay using 21F/40T (pol) and the exonuclease assay using 21F (exo) are given under Materials and methods section. (**B**) Time course analysis of polymerase activity in the presence of 5 mM $MgCl_2$ using 21F/40T. The reaction mixtures were supplemented with 10 μM dNTPs or NTPs as substrates. (**C**) Time course analysis of exonuclease activity in the presence of 1 mM $MnCl_2$ against ssDNA (21F) and dsDNA (21F/21R). (**D**) Single nucleotide insertion opposite dC in the presence of 5 mM $MgCl_2$ using 21F/40T. The substrates were in the triphosphate state and their concentrations were as follows: dG and rG, 1 μM; dNs and rNs, 10 μM; other nucleotides including damaged bases, 100 μM. Among the substrates, Ns, X, I and 8-OG stand for four NTP mixtures, xanthine, inosine and 8-oxo-dGTP, respectively. (**E**) TLS and RT assays. Reaction mixtures comprised 20 mM Tris–HCl, 20 mM KCl, 5 mM $MgCl_2$, 10 μM dNTPs or NTPs, 1 μM ttPolX, 10 nM 5′-labeled primer (9P) and 10 nM each template (21F, 12C21, 12I21, 12X21 or 21RNA), pH 8.0, at 37°C. The reaction mixtures were incubated for 30 min (A and D), 2 h (E) or as indicated in the figure (B and C) at 37°C, and then analyzed by 18% (A, B and D) or 20% (C and E) denaturing PAGE (8 M urea) and autoradiography. In the figure, 'd' and 'r' represents deoxyribonucleotide and ribonucleotide, respectively.

was hardly observed with 9P/21F and dNTPs as substrates at 25, 30 and 37°C (Figure 4E, lane 2). The first inserted bases were dT and dG for 9P/21F and 9P/2C21, respectively. When dTTP was the only available nucleotide, ttPolX was able to insert dTMP even with 9P/21F (Figure 4E, lane 1). These results suggest that ttPolX likely prefers dG to dT.

The activities of the ttPOLXc domain

We found that the ttPOLXc domain had Mg^{2+}-dependent DNA polymerase activity but no 3′–5′ exonuclease activity (Figure 5A). Furthermore, we observed Mn^{2+}-dependent DNA polymerase activity for the ttPOLXc domain under the polymerase assay conditions (Figure 5A, lane 2). This is probably because the ttPOLXc domain had no Mn^{2+}-dependent 3′–5′ exonuclease activity (Figure 5A, lane 4). The ttPOLXc domain exhibited no exonuclease activity in the presence of Mg^{2+} or Mn^{2+} (Figure 5A, lanes 3 and 4) as well as Zn^{2+}, Ni^{2+}, Ca^{2+} or Co^{2+} (data not shown). Time course analysis of the polymerase activity showed that the ttPOLXc domain had DNA/RNA polymerase activity dependent on both Mg^{2+} and Mn^{2+} (Figure 5B). The Mg^{2+}-dependent polymerase reaction was faster than the Mn^{2+}-dependent activity in the presence of 5 mM Mg^{2+} or 1 mM Mn^{2+}. The ttPOLXc domain showed faster polymerase reaction with Mg^{2+} than that of ttPolX (Figures 4B and 5B). The ttPOLXc domain exhibited no polymerase activity with 5 mM Zn^{2+}, Ni^{2+}, Ca^{2+} or Co^{2+}, or without a metal ion (data not shown).

We examined the ability of ttPOLXc domain to discriminate bases. In the presence of Mg^{2+} or Mn^{2+}, the ttPOLXc domain inserted dIMP, IMP and 8-oxo-dGMP opposite dC (Figure 5C) as well as dGMP and GMP (data not shown). Although ttPolX showed such insertion with Mg^{2+}, the ttPOLXc domain seemed to produce more extended primers (22-mer) (Figures 4D and 5C). The ttPOLXc domain did not insert dNMP or NMP opposite A in the template of 21RNA or dX in 12X21, but inserted dNMPs opposite dI in the template of 12I21 in the presence of Mg^{2+} or Mn^{2+} (Figure 5D), which was different from ttPolX (Figure 4E). Thus, the ttPOLXc domain had lower ability to discriminate base-pairing than that of ttPolX.

The activities of the ttPHP domain

The ttPHP domain exhibited no polymerase and no exonuclease activity with a cofactor of Mg^{2+} or Mn^{2+} (data not shown). The α-subunit of *T. thermophilus* PolIII also has a PHP domain at its N-terminus, and

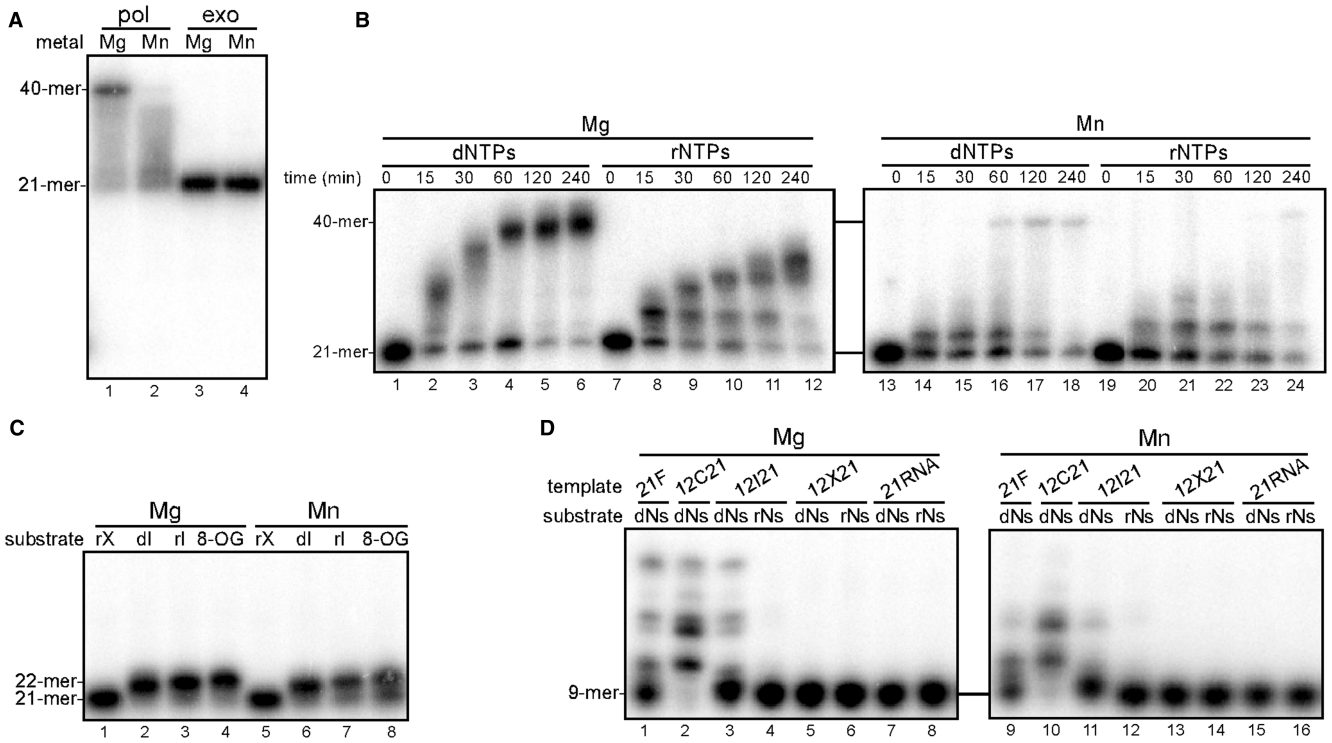

Figure 5. Mg^{2+}- and Mn^{2+}-dependent polymerase activity of the ttPOLXc domain. The measurement conditions were the same as given in Figure 4 except for the use of ttPOLXc domain. In these assays, 5 mM $MgCl_2$ or 1 mM $MnCl_2$ was used as a cofactor. (**A**) Metal ion dependence of the activities. (**B**) Time course analysis of polymerase activity. (**C**) Single nucleotide insertion opposite dC. (**D**) TLS and RT assays.

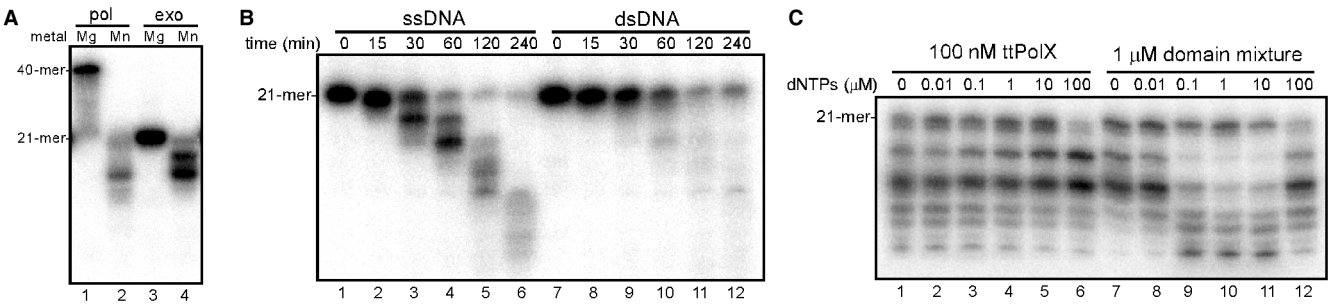

Figure 6. The activities of the mixture of the ttPOLXc and ttPHP domains. The measurement conditions were the same as given in Figure 4 except for the use of domain mixture (containing 1 μM ttPOLXc and 1 μM ttPHP domains). (**A**) Metal ion dependence of polymerase activity. (**B**) Time course analysis of exonuclease activity against ssDNA and dsDNA. (**C**) Exonuclease assay with dNTPs. Reaction mixtures comprised 20 mM Tris–HCl, 20 mM KCl, 1 mM $MnCl_2$, 100 nM ttPolX or 1 μM domain mixture, 10 nM 5′-labeled 21F and indicated amount of dNTPs, pH 8.0, at 37°C. The reaction mixtures were incubated for 30 min at 37°C, and then analyzed by 20% denaturing PAGE (8 M urea), but the running time was longer than that in (B). Note that the concentration of the domain mixture was higher than that of ttPolX.

has Zn^{2+}-dependent 3′–5′ exonuclease activity (24). We then performed the exonuclease assay with Zn^{2+} using the ttPHP domain, but observed no exonuclease activity (data not shown). This was an unexpected result because ttPolX had Mn^{2+}-dependent 3′–5′ exonuclease activity and the ttPOLXc domain had no exonuclease activity. CD spectra in the far-UV region indicated that the ttPHP domain was highly structured with a high content of α-helix (data not shown). Therefore, we concluded that the ttPHP domain has no intrinsic activity by itself under the conditions tested in this study.

The activities of a mixture of the ttPOLXc and ttPHP domains

A mixture of the ttPOLXc and ttPHP domains (domain mixture) had Mn^{2+}-dependent 3′–5′ exonuclease activity as well as Mg^{2+}-dependent DNA polymerase activity (Figure 6A). This metal ion selectivity of the activities was the same as that of ttPolX. These results suggest interaction between the ttPOLXc and ttPHP domains. Time course analysis of the exonuclease activity showed that the domain mixture was able to degrade both ssDNA and dsDNA but the activity for ssDNA was higher than that for dsDNA (Figure 6B). Furthermore, we

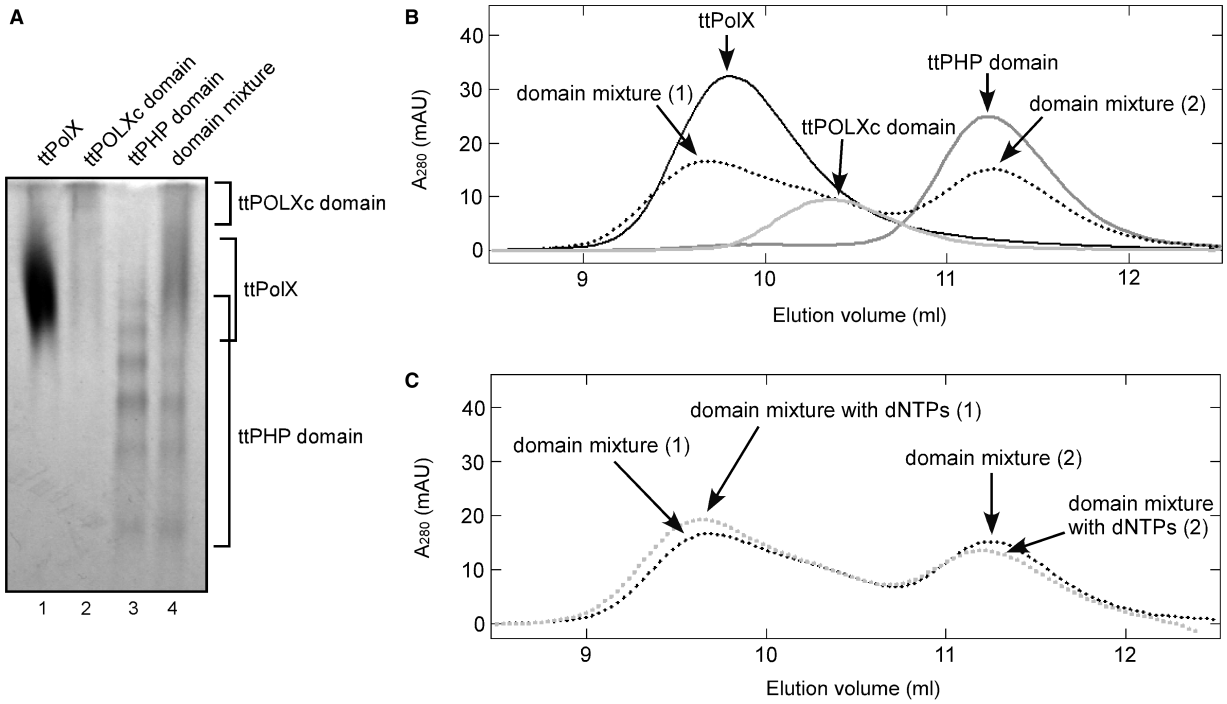

Figure 7. The interaction between the ttPOLXc and ttPHP domains. (**A**) Proteins were analyzed by 7.5% native PAGE and stained with CBB. The samples electrophoresed in the lanes were as follows: 1, 50 pmol ttPolX; 2, 50 pmol ttPOLXc domain; 3, 50 pmol ttPHP domain; and 4, 50 pmol ttPOLXc domain and 50 pmol ttPHP domain. The positions of the proteins on the gel are indicated on right side of the figure. (**B**) Elution profiles of ttPolX (black line), the ttPOLXc domain (light gray line), the ttPHP domain (dark gray line) and the domain mixture (dotted black line) on size exclusion chromatography. Proteins (500 pmol each) were incubated in buffer comprising 20 mM Tris–HCl and 100 mM KCl with or without 10 μM dNTPs, pH 8.0, at 37°C. The mixtures were incubated for 30 min at 37°C and then applied to a Superdex 75 column and eluted with incubation buffer. The elution volume, absorbance values and MWs estimated from the elution volume of each peak are summarized in Table 1. Arrows in the graph indicate the peaks in each elution profile. In the profile of the domain mixture, there were two main peaks. We named their peaks 1 and 2 in elution order. (**C**) Elution profiles of the domain mixture in the presence (dotted light gray line) and absence (dotted black line) of 10 μM dNTPs. The eluted peaks were named as described above.

found that the exonuclease activity of the domain mixture increased in the presence of 0.1–10 μM dNTPs, whereas that of ttPolX did not change with dNTPs (Figure 6C). We calculated steady-state kinetic parameters for the 3′–5′ exonuclease activity of ttPolX and the domain mixture against 3′-labeled 21-mer ssDNA (see Materials and methods section). The K_m values of ttPolX were 1700 (without dNTPs) and 1300 nM (with dNTPs), whereas those of the domain mixture were 770 (without dNTPs) and 530 nM (with dNTPs). The catalytic efficiencies (k_{cat}/K_m) of ttPolX were 2.8×10^4 (without dNTPs) and $3.8 \times 10^4\,s^{-1}M^{-1}$ (with dNTPs), whereas those of the domain mixture were 3.5×10^2 (without dNTPs) and $1.5 \times 10^3\,s^{-1}M^{-1}$ (with dNTPs). The catalytic efficiency of ttPolX was almost the same with and without dNTPs, whereas that of the domain mixture increased on the addition of dNTPs.

The interaction between the ttPOLXc and ttPHP domains

To verify whether the ttPOLXc and ttPHP domains interact with each other, we performed native PAGE. On the polyacrylamide gel, the ttPolX, ttPOLXc and ttPHP domains showed mobility corresponding to their pI values (Figure 7A): 6.26, 8.40 and 6.04, respectively. It was confirmed by PMF analysis that all bands in the lane of the ttPHP domain contained the ttPHP domain (Figure 7A, lane 3). In the lane of the domain mixture, the bands with the same mobility as ttPolX were apparently increased compared with the lanes of the ttPOLXc and ttPHP domains (Figure 7A). This mobility shift suggests interaction between the ttPOLXc and ttPHP domains.

We further examined this interaction by size exclusion chromatography (Figure 7B and Table 1). The ttPolX, ttPOLXc and ttPHP domains were eluted as single peaks at different elution volumes. When the ttPOLXc and ttPHP domains were mixed, a new peak appeared at 9.7 ml, which was different from those of the ttPOLXc and ttPHP domains. Concomitantly with the appearance of this peak, the peak of the ttPHP domain (11.3 ml) decreased. Since the peak of the ttPOLXc domain partially overlapped with that of 9.7 ml, we could not observe a clear peak of the ttPOLXc domain in the elution profile of the domain mixture. The elution volume of 9.7 ml (50 kDa) was very similar to that of ttPolX (9.8 ml, 48 kDa), suggesting that the peak eluted at 9.7 ml corresponded to a complex between the ttPOLXc and ttPHP domains in a 1:1 molar ratio. Based on the difference in the absorbance of the peaks corresponding to the ttPHP domains between the ttPHP domain alone and the domain mixture, ~40% of the ttPHP domain was assumed to form the complex (Table 1). Furthermore, we changed

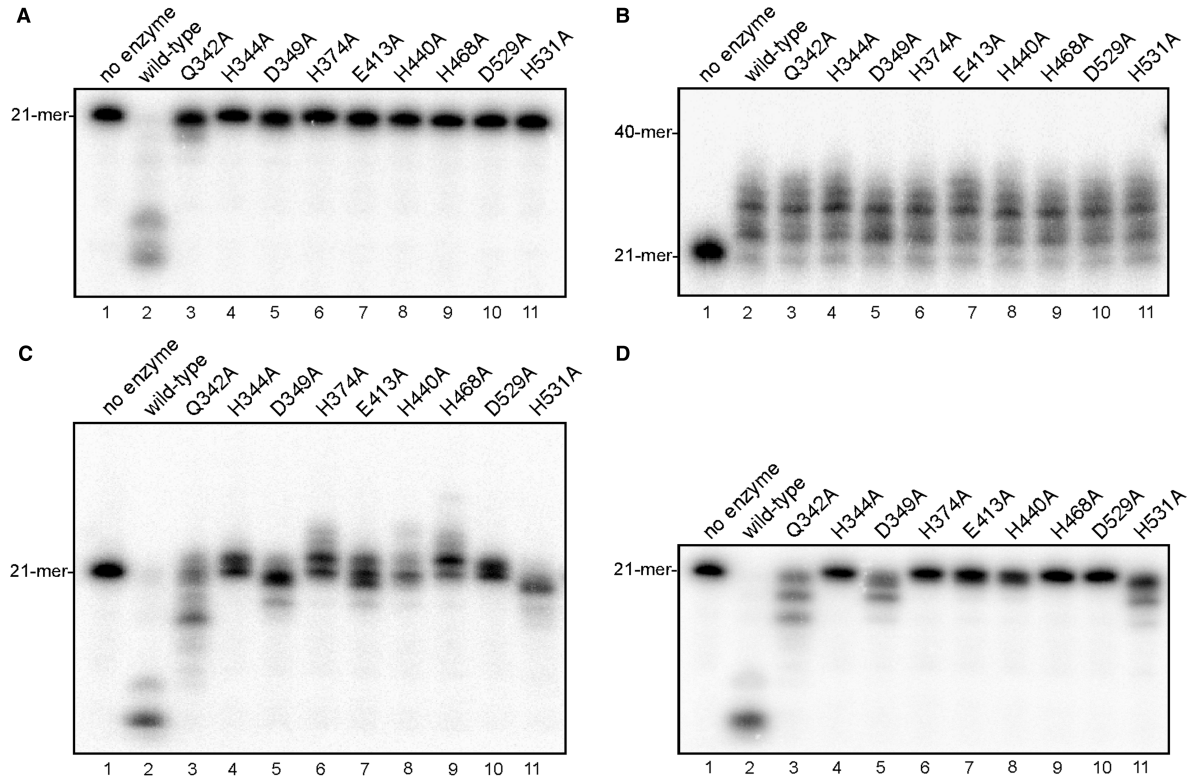

Figure 8. Site-directed mutagenesis of ttPolX. Reaction mixtures containing 1 μM wild-type ttPolX, a mutant or no enzyme were incubated for 30 min at 37°C. Exonuclease assays were performed in the absence (**A**) and presence (**D**) of 10 μM dNTPs (D). DNA polymerase assays were performed using 21F/40T and 10 μM dNTPs in the presence of 5 mM Mg^{2+} (**B**) or 1 mM Mn^{2+} (**C**). The reaction mixtures were analyzed by 18% (B) or 20% (A, C and D) denaturing PAGE (8 M urea) and autoradiography.

the ratio of domains for the domain mixture to 2:1 or 10:1 (Figure S1 and Table S1). When the domain ratio (ttPOLXc:ttPHP) was 10:1, most of the ttPHP domain appeared to form the complex with the ttPOLXc domain. SDS–PAGE analysis of the eluted fractions indicated that the early-eluting peak (10.0 ml) contained both ttPOLXc and ttPHP domains.

In the presence of dNTPs, the peak absorbance of the complex of the domains was 1.1-fold increased, whereas the peak absorbance of the ttPHP domain was 0.89-fold decreased (Figure 7C and Table 1). These results suggest that the complex of the domains was stabilized in the presence of dNTPs.

Site-directed mutagenesis of ttPolX

To investigate the involvement of the ttPHP domain in the exonuclease activity, the residues, Gln-342, His-344, Asp-349, His-374, Glu-413, His-440, His-468, Asp-529 and His-531, that were thought to bind to metal ions in the ttPHP domain, were substituted by alanine. These residues were selected based on the *E. coli* YcdX crystal structure (19), and sequence alignment between ttPolX and YcdX (Figure 3C). Glu-493 in the ttPHP domain is thought to contribute little to the catalytic reaction because the corresponding residue in YcdX (Glu-156) does not bind to a metal ion directly but stabilizes His-7 (19). Therefore, Glu-493 was excluded from the mutagenesis analysis. Mutations were confirmed by DNA sequencing and PMF with MALDI-TOF MS.

All nine mutations significantly decreased the Mn^{2+}-dependent 3′–5′ exonuclease activity (Figure 8A). In contrast, the Mg^{2+}-dependent DNA polymerase activity of all mutants was almost the same as that of wild-type ttPolX (Figure 8B). The latter observation coincides with the notion that DNA polymerase activity resides in the ttPOLXc domain. These results suggest that these residues are directly involved in the 3′–5′ exonuclease activity but not in the DNA polymerase activity.

The presence of dNTPs and of primer/template oligonucleotides promoted the Mn^{2+}-dependent 3′–5′ exonuclease activity of Q342A, D349A, E413A and H531A (Figure 8C and D). Since all mutants had weak or no 3′–5′ exonuclease activity, we thought these mutants exhibit Mn^{2+}-dependent DNA polymerase activity like the ttPOLXc domain. Under the polymerase assay conditions in the presence of Mn^{2+}, however, Q342A, D349A, E413A and H531A exhibited stronger 3′–5′ exonuclease activity (Figure 8C) than under the exonuclease assay conditions (Figure 8A). H344A, H374A, H440A, H468A and D529A exhibited Mn^{2+}-dependent DNA polymerase activity but no detectable Mn^{2+}-dependent 3′–5′ exonuclease activity, therefore, these mutants hardly exhibited the exonuclease activity even in the presence of dNTPs and primer/template oligonucleotides. The effect of dNTPs on the Mn^{2+}-dependent 3′–5′ exonuclease activity

was further investigated (Figure 8D). The Mn^{2+}-dependent 3′–5′ exonuclease activities of Q342A, D349A and H531A were promoted more in the presence of dNTPs than in the absence of dNTPs but less than in the presence of dNTPs and primer/template oligonucleotides (Figure 8A, C and D). Even when the reaction time was prolonged to 2 h in the exonuclease assay or the assay with dNTPs, the 3′–5′ exonuclease activities of H344A, H374A, H468A and D529A were hardly observed, but that of H440A was observed (data not shown). Therefore, we concluded that His-344, His-374, His-468 and Asp-529 of ttPolX are the most important residues for the 3′–5′ exonuclease activity.

DNA-binding abilities of ttPolX and its domains

Finally, we examined the DNA-binding abilities of ttPolX and its domains by means of EMSA. We used four DNAs of different structures: ssDNA, dsDNA, 1-nt gapped DNA and 5′-phosphorylated 1-nt gapped DNA. ttPolX and the ttPOLXc domain were able to bind to all DNA substrates but exhibited different binding properties for the four DNA structures (Figure 9A and B, and Table 2). ttPolX showed stronger binding ability as to gapped DNAs than ssDNA and dsDNA. The ttPOLXc domain showed weaker binding ability as to all DNA substrates than ttPolX (Figure 9A and B). Additionally, the ttPOLXc domain showed no significant difference in binding ability between gapped DNA and nongapped DNA. It should be mentioned that the binding curves were sigmoidal (Figure 9B). Assuming multiple molecules of a protein bind to DNA, we determined K_d^{app} and n (the number of bound protein) (see Materials and methods section). The ttPHP domain was unable to bind to all of the DNA structures, even though the concentration of ttPHP domain was 6.5 μM (Figure 9A and 9B). We observed more than two shifted bands in some lanes for ttPolX and the ttPOLXc domain. The appearance of multiple shifted bands and the n values suggest that more than two molecules of ttPolX or the ttPOLXc domain bound to a DNA. There was almost no difference between the binding abilities as to 5′-phosphorylated and unphosphorylated 1-nt gapped DNA (Figure 9A and B, and Table 2). Figure 9C shows that putative residues which recognize 5′-phosphate are conserved in various PolXs (see Discussion section).

DISCUSSION

The biochemical activities of ttPolX

This study revealed ttPolX has Mg^{2+}-dependent DNA/RNA polymerase activity and Mn^{2+}-dependent 3′–5′ exonuclease activity (Figure 4). Since the ttPOLXc domain has Mn^{2+}-dependent DNA/RNA polymerase activity (Figure 5), and the mutants lacking Mn^{2+}-dependent 3′–5′ exonuclease activity had Mn^{2+}-dependent DNA polymerase activity (Figure 8C), ttPolX probably also has Mn^{2+}-dependent DNA/RNA polymerase activity. This metal ion selectivity of the DNA/RNA polymerase activity is similar to those of Polλ and Polμ of the X-family (5,8,9). Our results indicate that the 3′–5′ exonuclease activity of ttPolX is much stronger than its polymerase activity in the presence of Mn^{2+} (Figure 4A). The 3′–5′ exonuclease activity of many DNA polymerases can be induced by either Mg^{2+} or Mn^{2+} (29). To the best of our knowledge, bacterial PolX is the first example of a DNA polymerase that has 3′–5′ exonuclease activity which requires only Mn^{2+} as a cofactor. This metal ion selectivity is similar to drPolX, a bacterial PolX having a PHP domain (22). However, the intracellular Mn^{2+} level of *D. radiodurans* is very high, and many enzymes are supposed to have Mn^{2+}-dependent activity (25). Therefore, the Mn^{2+}-dependent 3′–5′ exonuclease activity of drPolX does not simply apply to bacterial PolXs. In this study, we revealed ttPolX also has Mn^{2+}-dependent 3′–5′ exonuclease activity.

ttPolX had both ssDNA- and dsDNA-binding abilities (Figure 9B and Table 2). EMSA analysis suggested that more than two molecules of ttPolX bind to a 40-mer DNA with or without a 1-nt gap (Table 2). It was reported that rat Polβ formed a 2:1 Polβ–DNA complex in solution against 1-nt gapped 16-mer DNA when Polβ was in excess of DNA (30). Tang *et al*. also reported that more than two Polβ molecules bind to 45-mer 1-nt gapped DNA under the lower salt (~0.1 M KCl) conditions. This observation is in agreement with that for ttPolX. Although ttPolX has an additional domain, a PHP domain (Figure 1), the DNA-binding model of ttPolX is assumed to be the same as that of Polβ.

ttPolX preferred gapped DNA over non-gapped DNA, but did not recognize a 5′-phosphate group in the 1-nt gap (Figure 9 and Table 2). Some DNA polymerases involved in BER and DSBR prefer gapped DNA, especially 5′-phosphorylated gapped DNA, because these DNAs are some of the intermediates in these repair processes (31–33). The crystal structures of the complex of 5′-phosphorylated gapped DNA and Polβ (34), Polλ (35) or Polμ (36) revealed putative basic residues which recognize 5′-phosphate groups. Multiple sequence alignment of the POLXc domain regions of PolXs shows that three residues (B1–B3) are partially conserved (Figure 9C). It was reported that Polβ, Polλ, Polμ and spPolIV had higher gap-filling activity against a substrate containing 5′-phosphate group in the gap than a substrate without 5′-phosphate group (5,8,37,38) but scPolIV did not (39). ttPolX had little or no ability to recognize a 5′-phosphate group in the gap (Figure 9 and Table 2). Interestingly, ttPolX and scPolIV have Asp and Ser at the B2 position, respectively, whereas the other four PolXs have basic residues at the same position (Figure 9C). The distances between the oxygen atom of 5′-phosphate and nitrogen atoms of B1–B3 residues are as follows: Polβ, 2.73 (Lys-35), 2.60 (Lys-68) and 4.20 Å (Lys-72); Polλ, 2.95 (Arg-275), 2.84 (Arg-308) and 3.43 Å (Lys-312); Polμ, 3.65 (Arg-175) and 2.77 Å (His-208). Since B2 is the closest residue to the 5′-phosphate group in the three crystal structures, B2 is considered to be the critical residue for recognition of the 5′-phosphate group. Therefore, these results suggest that it is due to the lack of a basic residue at the B2 position that ttPolX and scPolIV cannot recognize a 5′-phosphate group (Figure 9C).

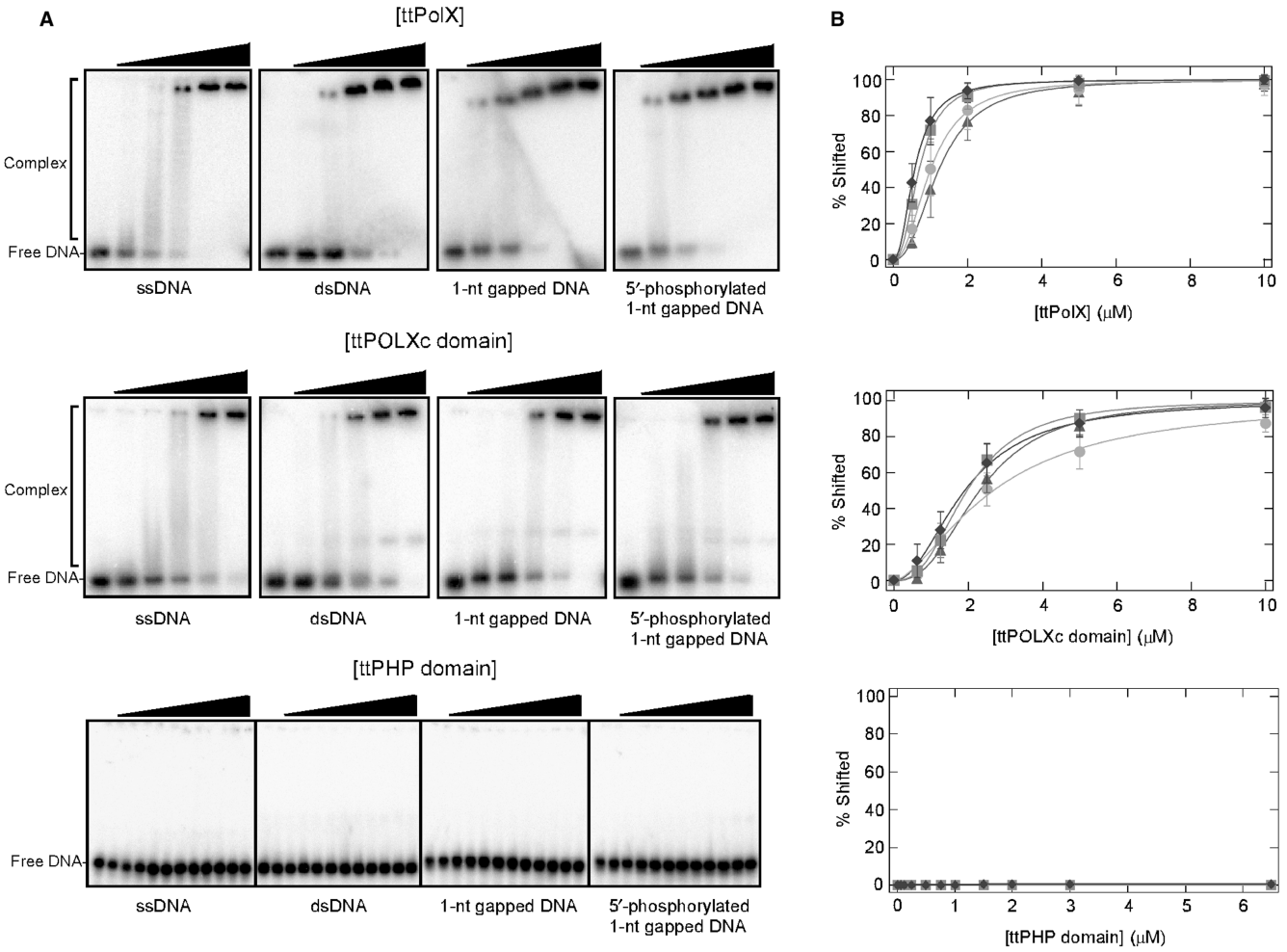

Figure 9. EMSA of ttPolX, and the ttPOLXc and ttPHP domains against four kinds of DNA. (**A**) Proteins were mixed with 10 nM each DNA and then analyzed by 5% PAGE. The concentrations of ttPolX were 0, 0.5, 1, 2, 5 and 10 μM. The concentrations of the ttPOLXc domain were 0, 0.625, 1.25, 2.5, 5 and 10 μM. The concentrations of the ttPHP domain were 0, 0.01, 0.0625, 0.125, 0.25, 0.5, 0.75, 1, 1.5, 2, 3 and 6.5 μM. (**B**) The percentage of the protein–DNA complex was determined and plotted against the protein concentration. The symbols were as follows: circles, ssDNA; squares, dsDNA; triangles, 1-nt gapped DNA; diamonds, 5′-phosphorylated 1-nt gapped DNA. The data were fitted with equation (4) using Igor 4.03. Data represent the means for four or five independent experiments ± standard deviation. (**C**) Sequence alignment of the POLXc domain regions of PolXs. White letters in black boxes indicate putative residues interacting with 5′-phosphate in the crystal structures of hsPolμ (PDB ID: 2fms), hsPolλ (PDB ID: 1xsn) and mmPolμ (PDB ID: 2ihm). The residues with a gray background are putative residues interacting with 5′-phosphate predicted from the alignment. B1, B2 and B3 represent the positions of the basic amino acid residues. The alignment was performed with ClustalW2 (28). The accession numbers were as follows: NP_002681 for *H. sapiens* Polβ (hsPolβ); NP_037406 for *H. sapiens* Polλ (hsPolλ); NP_059097 for *Mus musculus* Polμ (mmPolμ); NP_009940 for *Saccharomyces cerevisiae* PolIV (scPolIV); NP_592977 for *Schizosaccharomyces pombe* PolIV (spPolIV); and YP_144416 for *T. thermophilus* HB8 PolX (ttPolX).

As seen in the assay of single nucleotide insertion, ttPolX inserted dGMP, GMP and 8-oxo-dGMP and slightly inserted dIMP and IMP opposite dC (Figure 4D). Such an ability of ttPolX to discriminate base-pairing is similar to those of Polβ, Polλ and Polμ of the mammalian PolXs on single nucleotide insertion when the frameshift DNA synthesis is not taken into consideration (40–42). ttPolX exhibited no detectable TLS against xanthine or inosine, or RT activity in the presence of Mg^{2+} (Figure 4E). Note that ttPolX exhibited

Table 2. Comparison of DNA-binding abilities of ttPolX and its domains

	ssDNA[a]		dsDNA[b]		1-nt gapped DNA[b]		5′-phosphorylated 1-nt gapped DNA[a]	
	K_d^{app} (μM)	*n*	K_d^{app} (μM)	*n*	K_d^{app} (μM)	*n*	K_d^{app} (μM)	*n*
ttPolX	1.2 ± 0.70	2.4 ± 0.74	1.2 ± 0.70	2.5 ± 0.57	0.39 ± 0.15	2.3 ± 0.46	0.30 ± 0.18	2.4 ± 1.0
ttPOLXc domain	5.5 ± 1.7	1.7 ± 0.29	9.3 ± 3.8	2.6 ± 0.23	6.5 ± 2.5	2.5 ± 0.65	4.8 ± 2.5	2.3 ± 1.0
ttPHP domain	N.D.	N.D.	N.D.	N.D.	N.D.	N.D.	N.D.	N.D.

N.D.: not detected.
[a]Data represent the means for five independent experiments ± standard deviation.
[b]Data represent the means for four independent experiments ± standard deviation.

no 3′–5′ exonuclease activity in these assays because it exhibited no exonuclease activity with Mg^{2+}. Several PolXs such as Polλ and Polμ are called translesion or error-prone DNA polymerases because they insert incorrect bases including damaged ones or carrying out TLS against a damaged base or a mismatched base (40,42,43). However, ttPolX is unlikely to be a translesion DNA polymerase.

The RNA polymerase activity of ttPolX may help to repair DNA. ttPolX was able to insert NMPs opposite a DNA template (Figure 4B). Some PolXs such as Polβ and Polμ are also capable of incorporating NMPs (38). It was reported that the intracellular NTPs concentration was much higher than that of dNTPs in human cell lines (44) and in *E. coli* cells (45). It is perhaps an advantage for repairing DNA that ttPolX can use NTPs, which exist at high concentrations in the cell, especially when the intracellular dNTP concentration is low. The nucleotide concentration is known to decrease in the stationary phase, but even in such a phase, the NTP concentration is still higher than that of dNTP (45). *Thermus thermophilus* HB8 has a junction ribonuclease, which recognizes the RNA–DNA junction of an RNA–DNA/DNA heteroduplex and cleaves it leaving a mono-ribonucleotide at the 5′ terminus of the RNA–DNA junction (46). Incorporated NMP in DNA could serve as a 'flag waver' and be recognized by enzymes, such as a junction ribonuclease and induce an additional DNA repair system or DNA damage checkpoint pathways (28).

Site-directed mutagenesis revealed that Gln-342, His-344, Asp-349, His-374, Glu-413, His-440, His-468, Asp-529 and His-531 in ttPolX are important residues for the 3′–5′ exonuclease activity (Figure 8). Among these residues, His-344, His-374, His-468 and Asp-529 are essential for the activity. In the YcdX crystal structure, the corresponding residues, His-9, His-40, His-131 and Asp-192 (Figure 3C) (19), are coordinated to bound Zn 2, Zn 1, Zn 3 and Zn 2 in a trinuclear zinc cluster, respectively. Thus, ttPolX may have three metal ions, which are equally important for catalysis, in the active site of the PHP domain. It is possible to suppose that the mechanism underlying the 3′–5′ exonuclease activity is similar to that of endonuclease IV, a DNA repair enzyme which has a TIM barrel fold, similar to that of YcdX and utilizes a three metal ion catalytic mechanism (47). It should be mentioned here that dNTPs promoted the 3′–5′ exonuclease activity of several mutants (Figure 8C and D). Assuming that dNTPs bind to the POLXc domain, it is possible that the observed promotion was triggered by a conformational change of the ttPOLXc domain. If the ttPOLXc domain is involved in binding to ssDNA (see below), binding of dNTP might increase the affinity to ssDNA, leading to promotion of the exonuclease activity. It should be mentioned, however, that dNTPs did not significantly stimulate the exonuclease activity of ttPolX (Figure 6C). Alternatively, a conformational change of the ttPHP domain might be caused through the interaction with the ttPOLXc domain (see below).

ttPolX mainly consists of POLXc and PHP domains

Many bacterial PolXs including ttPolX have been predicted to consist of mainly two domains, POLXc and PHP domains (Figure 1). The POLXc domain is a polymerase domain, whereas the PHP domain is predicted to be a phosphoesterase domain. The PHP domain is associated with other domains, such as the polymerase domain (20,21) or exists as a stand-alone protein (19,48). We could identify ttPOLXc and ttPHP domains in ttPolX experimentally and purify them (Figures 1–3).

Although the ttPOLXc domain inserted dGMP, GMP, dIMP, IMP and 8-oxo-dGMP opposite dC (Figure 5C), the incorporation rate of damaged bases with the ttPOLXc domain was higher than that in the case of ttPolX. This enhancement of the rate cannot be explained only by the higher polymerase activity than that of ttPolX. Moreover, the ttPOLXc domain differed from ttPolX in that this domain exhibited TLS activity opposite dI (Figure 5D). It is probable that the ttPHP domain represses the incorporation of NTPs, especially damaged bases, directly or indirectly. The ttPHP domain may improve the stringency of base paring.

When the ttPOLXc and ttPHP domains were mixed, the domain mixture showed both DNA polymerase and 3′–5′ exonuclease activities. The metal ion selectivity of these activities was the same as that of ttPolX (Figure 6A). The higher 3′–5′ exonuclease activity of the domain mixture as to ssDNA than to dsDNA was also the same as that of ttPolX (Figure 6B). These results suggest the domains formed a complex which has the same properties as ttPolX. The reason why the 3′–5′ exonuclease activity of the domain mixture was lower than that of ttPolX is probably that not all the ttPOLXc and ttPHP domains formed

the complex. This is supported by the results of native PAGE and size exclusion chromatography (Figure 7).

We detected an interaction between the ttPOLXc and ttPHP domains. On the native PAGE gel (Figure 7A), the domain mixture showed a smear band exhibiting a similar mobility to ttPolX. This result suggests the two domains formed a complex with a similar surface charge and/or a similar overall shape to ttPolX. The smear band of ttPolX may be due to a nonuniform distribution of the surface charge or structural fluctuation of the ttPolX. The appearance of many bands of the ttPHP domain indicates this domain existed in several different states. However, size exclusion chromatography revealed that the ttPHP domain existed in a monomeric state (Figure 7B). Therefore, the observed multiple bands of the ttPHP domain may not mean different assembly states of the ttPHP domain. A further experiment on the domain interaction involving size exclusion chromatography suggested that the ttPOLXc domain bound to the ttPHP domain in the ratio of 1:1 (Figure 7B and Table 1). Since it is considered that the POLXc and PHP domains are linked through an interdomain linker, the observed interaction between the separate domains is assumed to occur also between the domains in the ttPolX molecule. It was reported that the N-terminal PHP domain of the α-subunit of *E. coli* PolIII binds to the ε-proofreading subunit (49). This raises the possibility that the PHP domain is a platform enabling coordination of proofreading and polymerase activities during chromosomal replication. There are two ε-subunits in *T. thermophilus* HB8 cells, TTHA0574 (probable PolIII ε-subunit) and TTHA0813 (PolIII ε-chain-like protein). These proteins exhibit 33 and 31% amino acid identity to the ε-subunit of the *E. coli* PolIII, respectively. ttPolX may be able to bind to these proteins through the ttPHP domain, implying that ttPolX may be associated with a DNA 'replisome' or 'repairsome'.

In the presence of dNTPs, the complex of domains was slightly stabilized, and 3′–5′ exonuclease activity was significantly increased (Figures 6C and 7C). Since dNTP is a substrate for DNA polymerases, conformation of the ttPOLXc domain may change on the binding dNTPs to a form in which the ttPOLXc domain can interact with the ttPHP domain more strongly. The addition of dNTPs increased the complex of the domains by 10% (Figure 7C and Table 1), whereas it increased the catalytic efficiency of the 3′–5′ exonuclease activity 4-fold (Figure 6C). Since the size exclusion chromatography was performed in the absence of DNA, the binding of both DNA and dNTPs probably stabilized the domain complex much more than the binding of dNTPs alone. The crystal structure of the complex of Polβ with DNA revealed that in subdomains of the POLXc domain the conformational change induced by binding of DNA occurs in a distinct region from that induced by binding of dNTPs (30). ttPolX did not show an increase in the 3′–5′ exonuclease activity on the addition of dNTPs (Figure 6C). Since the POLXc and PHP domains are close to each other in the ttPolX molecule, the addition of dNTPs may not stabilize the domain interaction further.

The ttPOLXc domain also exhibited both ssDNA- and dsDNA-binding abilities by itself (Figure 9), and showed a similar DNA-binding manner to that of ttPolX (Table 2). Analysis of the binding curve suggested that more than two molecules of the ttPOLXc domain bound to a 40-mer DNA with or without a 1-nt gap, which is similar to the result for ttPolX (Table 2). These results indicate that the ttPOLXc domain in ttPolX mainly contributes to the binding to DNA. Indeed, the subdomains, which exhibit binding activity as to ssDNA or dsDNA, both belong to the POLXc domain in Polβ (15). However, the ttPOLXc domain exhibited lower affinity (higher K_d^{app} values) to DNA than ttPolX. The ttPHP domain may stabilize the ttPolX–DNA complex without affecting the DNA-binding manner, although the ttPHP domain has no DNA-binding ability. The contribution of the ttPHP domain to the affinity to DNA is probably auxiliary.

The ttPHP domain is essential for 3′–5′ exonuclease activity but has no intrinsic activity by itself

Our study demonstrated that the ttPHP domain was essential for the 3′–5′ exonuclease activity of ttPolX. This is inconsistent with the results for drPolX, which showed that the POLXc domain had 3′–5′ exonuclease activity (23). The observation that the PHP domain had no intrinsic activity is common to both ttPolX and drPolX. However, the ttPOLXc domain showed no exonuclease activity. As the POLXc domain of drPolX is homologous to that of ttPolX (and other PolXs), it seems difficult to explain this discrepancy. The PHP domain is present in organisms ranging from archaea and bacteria to fungi. The conserved residues in the PHP family are similar to those in the metal-dependent amidohydrolase superfamily, which includes the TatD-related DNase and phosphotriesterase families (18). The enzymes belonging to this superfamily have a metal-binding site where a metal-activated water molecule acts as a nucleophile for hydrolysis of the substrate. Therefore, the PHP domain is also thought to be a phosphoesterase domain (18). Actually, histidinol phosphate phosphatase belonging to the PHP domain family possesses phosphatase activity (48,50). We concluded that the ttPHP domain alone has no intrinsic 3′–5′ exonuclease activity, but is required for the activity of ttPolX.

Three possible reasons why the ttPHP domain has no intrinsic exonuclease activity by itself are as follows: (i) The ttPHP domain has almost all the catalytic residues required for 3′–5′ exonuclease activity but has no nuclease activity due to its inability to bind DNA. Alignment showed that the ttPHP domain in ttPolX has all putative catalytic residues, except for Gln-342, interacting with three zinc ions in the YcdX crystal structure (Figure 3C). Site-directed mutagenesis showed that all these residues are catalytically important for 3′–5′ exonuclease activity (Figure 8A). Therefore, it seems reasonable to speculate that the ttPHP domain has no 3′–5′ exonuclease activity because it cannot gain access to DNA with any structures (Table 2). As already described, the ttPOLXc domain possesses DNA-binding ability by itself. Furthermore, the tight interaction between the

ttPOLXc and ttPHP domains in the domain mixture (Figure 7) suggests that the two domains also tightly interact with each other within the ttPolX molecule. If this is the case, it is probable that the ttPHP domain requires proper interaction with the ttPOLXc domain as a substrate-binding unit to express its exonuclease activity. Indeed, the α-subunit of *T. thermophilus* PolIII, having Zn^{2+}-dependent 3′–5′ exonuclease activity (24), contains a DNA-binding domain besides the PHP domain; (ii) the ttPOLXc domain has some of the catalytic residues required for 3′–5′ exonuclease activity. The strong interaction of the ttPOLXc domain with the ttPHP domain (Figure 7) raises the possibility that these domains interact with each other via a large interface area within ttPolX. If the active site of the ttPHP domain is located proximately to the ttPOLXc domain, some residues of the ttPOLXc domain may serve as catalytic residues. It should be noted, however, that the sequence of the POLXc domain contains no known nuclease motif; (iii) the ttPHP domain is converted into an active form through interaction with the ttPOLXc domain. If this is true, it seems reasonable that the ttPHP domain alone had no intrinsic activity. In the case of the α-subunit of *E. coli* PolIII, deletion of the N-terminal 60 residues of the PHP domain abolishes both ε-binding and polymerase activity (49). A proper interaction between the PHP and polymerase domains may be important for maintaining the active forms of both domains. Combinations of the above three reasons are also possible.

In conclusion, our attempt to identify the functional domains of ttPolX revealed that the ttPHP domain has no intrinsic activity by itself but can interact with the ttPOLXc domain, and exhibits the 3′–5′ exonuclease activity. Our findings will provide an insight into the functions of bacterial conserved PolXs including a PHP domain.

NOTE IN PROOF

Our results are supported by two articles published just after our work had been completed. Baños *et al.* (51) revealed that PolX from *Bacillus subtilis* (PolXBs) has intrinsic 3′–5′ exonuclease activity, specialized in resecting unannealed 3′-termini, and the activity is resided in the PHP domain of PolXBs. Baños *et al.* (52) also showed that two evolutionary conserved residues located in the PHP domain are directly involved in 3′–5′ exonuclease activity. PolXBs is also a DNA polymerase, preferentially acting on DNA structure containing gap (52). Based on these results, Baños *et al.* (51,52) speculated that PolXBs are involved in DNA repair, especially in BER. The facts that ttPolX has 37% amino acids identity to PolXBs and similar biochemical activities imply that ttPolX may also be involved in such a DNA repair process.

SUPPLEMENTARY DATA

Supplementary Data is available at NAR Online.

ACKNOWLEDGEMENTS

The authors thank Yumiko Inoue for the technical assistance in the peptide sequencing and Hirofumi Omori for the technical assistance in the DNA sequencing.

FUNDING

Grants-in-Aid for Scientific Research 17770089 (to N.N.) and 20570131 (to R.M.) from the Ministry of Education, Science, Sports and Culture of Japan. Funding for open access charge: Grants-in-Aid for Scientific Research from the Ministry of Education, Science, Sports and Culture of Japan.

Conflict of interest statement. None declared.

REFERENCES

1. Rothwell,P.J. and Waksman,G. (2005) Structure and mechanism of DNA polymerases. *Adv. Protein Chem.*, **71**, 401–440.
2. Ramadan,K., Shevelev,I. and Hubscher,U. (2004) The DNA-polymerase-X family: controllers of DNA quality? *Nat. Rev. Mol. Cell Biol.*, **5**, 1038–1043.
3. Bergoglio,V., Ferrari,E., Hubscher,U., Cazaux,C. and Hoffmann,J.S. (2003) DNA polymerase β can incorporate ribonucleotides during DNA synthesis of undamaged and CPD-damaged DNA. *J. Mol. Biol.*, **331**, 1017–1023.
4. Srivastava,D.K., Berg,B.J., Prasad,R., Molina,J.T., Beard,W.A., Tomkinson,A.E. and Wilson,S.H. (1998) Mammalian abasic site base excision repair. Identification of the reaction sequence and rate-determining steps. *J. Biol. Chem.*, **273**, 21203–21209.
5. Garcia-Diaz,M., Bebenek,K., Sabariegos,R., Dominguez,O., Rodriguez,J., Kirchhoff,T., Garcia-Palomero,E., Picher,A.J., Juarez,R., Ruiz,J.F. *et al.* (2002) DNA polymerase λ, a novel DNA repair enzyme in human cells. *J. Biol. Chem.*, **277**, 13184–13191.
6. Ramadan,K., Maga,G., Shevelev,I.V., Villani,G., Blanco,L. and Hubscher,U. (2003) Human DNA polymerase λ possesses terminal deoxyribonucleotidyl transferase activity and can elongate RNA primers: implications for novel functions. *J. Mol. Biol.*, **328**, 63–72.
7. Capp,J.P., Boudsocq,F., Bertrand,P., Laroche-Clary,A., Pourquier,P., Lopez,B.S., Cazaux,C., Hoffmann,J.S. and Canitrot,Y. (2006) The DNA polymerase λ is required for the repair of non-compatible DNA double strand breaks by NHEJ in mammalian cells. *Nucleic Acids Res.*, **34**, 2998–3007.
8. Nick McElhinny,S.A. and Ramsden,D.A. (2003) Polymerase mu is a DNA-directed DNA/RNA polymerase. *Mol. Cell Biol.*, **23**, 2309–2315.
9. Dominguez,O., Ruiz,J.F., Lain de Lera,T., Garcia-Diaz,M., Gonzalez,M.A., Kirchhoff,T., Martinez,-A.C., Bernad,A. and Blanco,L. (2000) DNA polymerase mu (Pol μ), homologous to TdT, could act as a DNA mutator in eukaryotic cells. *EMBO J.*, **19**, 1731–1742.
10. Capp,J.P., Boudsocq,F., Besnard,A.G., Lopez,B.S., Cazaux,C., Hoffmann,J.S. and Canitrot,Y. (2007) Involvement of DNA polymerase μ in the repair of a specific subset of DNA double-strand breaks in mammalian cells. *Nucleic Acids Res.*, **35**, 3551–3560.
11. Bertocci,B., De Smet,A., Berek,C., Weill,J.C. and Reynaud,C.A. (2003) Immunoglobulin κ light chain gene rearrangement is impaired in mice deficient for DNA polymerase mu. *Immunity*, **19**, 203–211.
12. Boule,J.B., Rougeon,F. and Papanicolaou,C. (2001) Terminal deoxynucleotidyl transferase indiscriminately incorporates ribonucleotides and deoxyribonucleotides. *J. Biol. Chem.*, **276**, 31388–31393.

13. Carson,D.R. and Christman,M.F. (2001) Evidence that replication fork components catalyze establishment of cohesion between sister chromatids. *Proc. Natl Acad. Sci. USA*, **98**, 8270–8275.
14. Aravind,L. and Koonin,E.V. (1999) DNA polymerase β-like nucleotidyltransferase superfamily: identification of three new families, classification and evolutionary history. *Nucleic Acids Res.*, **27**, 1609–1618.
15. Beard,W.A. and Wilson,S.H. (2006) Structure and mechanism of DNA polymerase β. *Chem. Rev.*, **106**, 361–382.
16. Bork,P., Hofmann,K., Bucher,P., Neuwald,A.F., Altschul,S.F. and Koonin,E.V. (1997) A superfamily of conserved domains in DNA damage-responsive cell cycle checkpoint proteins. *FASEB J.*, **11**, 68–76.
17. Ma,Y., Lu,H., Tippin,B., Goodman,M.F., Shimazaki,N., Koiwai,O., Hsieh,C.L., Schwarz,K. and Lieber,M.R. (2004) A biochemically defined system for mammalian nonhomologous DNA end joining. *Mol. Cell*, **16**, 701–713.
18. Aravind,L. and Koonin,E.V. (1998) Phosphoesterase domains associated with DNA polymerases of diverse origins. *Nucleic Acids Res.*, **26**, 3746–3752.
19. Teplyakov,A., Obmolova,G., Khil,P.P., Howard,A.J., Camerini-Otero,R.D. and Gilliland,G.L. (2003) Crystal structure of the *Escherichia coli* YcdX protein reveals a trinuclear zinc active site. *Proteins*, **51**, 315–318.
20. Lamers,M.H., Georgescu,R.E., Lee,S.G., O'Donnell,M. and Kuriyan,J. (2006) Crystal structure of the catalytic α subunit of E. coli replicative DNA polymerase III. *Cell*, **126**, 881–892.
21. Bailey,S., Wing,R.A. and Steitz,T.A. (2006) The structure of *T. aquaticus* DNA polymerase III is distinct from eukaryotic replicative DNA polymerases. *Cell*, **126**, 893–904.
22. Lecointe,F., Shevelev,I.V., Bailone,A., Sommer,S. and Hubscher,U. (2004) Involvement of an X family DNA polymerase in double-stranded break repair in the radioresistant organism *Deinococcus radiodurans*. *Mol. Microbiol.*, **53**, 1721–1730.
23. Blasius,M., Shevelev,I., Jolivet,E., Sommer,S. and Hubscher,U. (2006) DNA polymerase X from *Deinococcus radiodurans* possesses a structure-modulated 3′→5′ exonuclease activity involved in radioresistance. *Mol. Microbiol.*, **60**, 165–176.
24. Stano,N.M., Chen,J. and McHenry,C.S. (2006) A coproofreading Zn^{2+}-dependent exonuclease within a bacterial replicase. *Nat. Struct. Mol. Biol.*, **13**, 458–459.
25. Daly,M.J., Gaidamakova,E.K., Matrosova,V.Y., Vasilenko,A., Zhai,M., Venkateswaran,A., Hess,M., Omelchenko,M.V., Kostandarithes,H.M., Makarova,K.S. *et al.* (2004) Accumulation of Mn(II) in *Deinococcus radiodurans* facilitates gamma-radiation resistance. *Science*, **306**, 1025–1028.
26. Zahradka,K., Slade,D., Bailone,A., Sommer,S., Averbeck,D., Petranovic,M., Lindner,A.B. and Radman,M. (2006) Reassembly of shattered chromosomes in *Deinococcus radiodurans*. *Nature*, **443**, 569–573.
27. Kuramitsu,S., Hiromi,K., Hayashi,H., Morino,Y. and Kagamiyama,H. (1990) Pre-steady-state kinetics of *Escherichia coli* aspartate aminotransferase catalyzed reactions and thermodynamic aspects of its substrate specificity. *Biochemistry*, **29**, 5469–5476.
28. Larkin,M.A., Blackshields,G., Brown,N.P., Chenna,R., McGettigan,P.A., McWilliam,H., Valentin,F., Wallace,I.M., Wilm,A., Lopez,R. *et al.* (2007) Clustal W and Clustal X version 2.0. *Bioinformatics*, **23**, 2947–2948.
29. Lin,T.C., Wang,C.X., Joyce,C.M. and Konigsberg,W.H. (2001) 3′-5′ Exonucleolytic activity of DNA polymerases: structural features that allow kinetic discrimination between ribo- and deoxyribonucleotide residues. *Biochemistry*, **40**, 8749–8755.
30. Tang,K.H., Niebuhr,M., Aulabaugh,A. and Tsai,M.D. (2008) Solution structures of 2 : 1 and 1 : 1 DNA polymerase-DNA complexes probed by ultracentrifugation and small-angle X-ray scattering. *Nucleic Acids Res.*, **36**, 849–860.
31. Hegde,M.L., Hazra,T.K. and Mitra,S. (2008) Early steps in the DNA base excision/single-strand interruption repair pathway in mammalian cells. *Cell Res.*, **18**, 27–47.
32. Pitcher,R.S., Brissett,N.C. and Doherty,A.J. (2007) Nonhomologous end-joining in bacteria: a microbial perspective. *Annu. Rev. Microbiol.*, **61**, 259–282.
33. Moon,A.F., Garcia-Diaz,M., Batra,V.K., Beard,W.A., Bebenek,K., Kunkel,T.A., Wilson,S.H. and Pedersen,L.C. (2007) The X family portrait: structural insights into biological functions of X family polymerases. *DNA Repair (Amst)*, **6**, 1709–1725.
34. Batra,V.K., Beard,W.A., Shock,D.D., Krahn,J.M., Pedersen,L.C. and Wilson,S.H. (2006) Magnesium-induced assembly of a complete DNA polymerase catalytic complex. *Structure*, **14**, 757–766.
35. Garcia-Diaz,M., Bebenek,K., Krahn,J.M., Kunkel,T.A. and Pedersen,L.C. (2005) A closed conformation for the Pol λ catalytic cycle. *Nat. Struct. Mol. Biol.*, **12**, 97–98.
36. Moon,A.F., Garcia-Diaz,M., Bebenek,K., Davis,B.J., Zhong,X., Ramsden,D.A., Kunkel,T.A. and Pedersen,L.C. (2007) Structural insight into the substrate specificity of DNA Polymerase μ. *Nat. Struct. Mol. Biol.*, **14**, 45–53.
37. Alonso,A., Terrados,G., Picher,A.J., Giraldo,R., Blanco,L. and Larraga,V. (2006) An intrinsic 5′-deoxyribose-5-phosphate lyase activity in DNA polymerase beta from *Leishmania infantum* supports a role in DNA repair. *DNA Repair (Amst)*, **5**, 89–101.
38. Gonzalez-Barrera,S., Sanchez,A., Ruiz,J.F., Juarez,R., Picher,A.J., Terrados,G., Andrade,P. and Blanco,L. (2005) Characterization of SpPol4, a unique X-family DNA polymerase in *Schizosaccharomyces pombe*. *Nucleic Acids Res.*, **33**, 4762–4774.
39. Bebenek,K., Garcia-Diaz,M., Patishall,S.R. and Kunkel,T.A. (2005) Biochemical properties of *Saccharomyces cerevisiae* DNA polymerase IV. *J. Biol. Chem.*, **280**, 20051–20058.
40. Brown,J.A., Duym,W.W., Fowler,J.D. and Suo,Z. (2007) Single-turnover kinetic analysis of the mutagenic potential of 8-oxo-7,8-dihydro-2′-deoxyguanosine during gap-filling synthesis catalyzed by human DNA polymerases λ and β. *J. Mol. Biol.*, **367**, 1258–1269.
41. Fiala,K.A., Duym,W.W., Zhang,J. and Suo,Z. (2006) Up-regulation of the fidelity of human DNA polymerase λ by its non-enzymatic proline-rich domain. *J. Biol. Chem.*, **281**, 19038–19044.
42. Zhang,Y., Wu,X., Yuan,F., Xie,Z. and Wang,Z. (2001) Highly frequent frameshift DNA synthesis by human DNA polymerase μ. *Mol. Cell Biol.*, **21**, 7995–8006.
43. Covo,S., Blanco,L. and Livneh,Z. (2004) Lesion bypass by human DNA polymerase μ reveals a template-dependent, sequence-independent nucleotidyl transferase activity. *J. Biol. Chem.*, **279**, 859–865.
44. Huang,D., Zhang,Y. and Chen,X. (2003) Analysis of intracellular nucleoside triphosphate levels in normal and tumor cell lines by high-performance liquid chromatography. *J. Chromatogr. B*, **784**, 101–109.
45. Buckstein,M.H., He,J. and Rubin,H. (2008) Characterization of nucleotide pools as a function of physiological state in *Escherichia coli*. *J. Bacteriol.*, **190**, 718–726.
46. Ohtani,N., Tomita,M. and Itaya,M. (2008) Junction ribonuclease: a ribonuclease HII orthologue from *Thermus thermophilus* HB8 prefers the RNA-DNA junction to the RNA/DNA heteroduplex. *Biochem. J.*, **412**, 517–526.
47. Ivanov,I., Tainer,J.A. and McCammon,J.A. (2007) Unraveling the three-metal-ion catalytic mechanism of the DNA repair enzyme endonuclease IV. *Proc. Natl Acad. Sci. USA*, **104**, 1465–1470.
48. Omi,R., Goto,M., Miyahara,I., Manzoku,M., Ebihara,A. and Hirotsu,K. (2007) Crystal structure of monofunctional histidinol phosphate phosphatase from *Thermus thermophilus* HB8. *Biochemistry*, **46**, 12618–12627.
49. Wieczorek,A. and McHenry,C.S. (2006) The NH_2-terminal php domain of the α subunit of the *Escherichia coli* replicase binds the epsilon proofreading subunit. *J. Biol. Chem.*, **281**, 12561–12567.
50. le Coq,D., Fillinger,S. and Aymerich,S. (1999) Histidinol phosphate phosphatase, catalyzing the penultimate step of the histidine biosynthesis pathway, is encoded by *ytvP* (*hisJ*) in *Bacillus subtilis*. *J. Bacteriol.*, **181**, 3277–3280.
51. Baños,B., Lázaro,J.M., Villar,L., Salas,M. and de Vega,M. (2008) Editing of misaligned 3′-termini by an intrinsic 3′-5′ exonuclease activity residing in the PHP domain of a family X DNA polymerase. *Nucl. Acids Res.*, **36**, 5736–5749.
52. Baños,B., Lázaro,J.M., Villar,L., Salas,M. and de Vega,M. (2008) Characterization of a Bacillus subtilis 64-kDa DNA Polymerase X potentially involved in DNA repair. *J. Mol. Biol.*, **384**, 1019–1028.